Colloids and Surfaces B: Biointerfaces 153 (2017) 229–236

Contents lists available at ScienceDirect

Colloids and Surfaces B: Biointerfaces

journal homepage: www.elsevier.com/locate/colsurfb

Full Length Article

The pH sensitive properties of carboxymethyl chitosan nanoparticles cross-linked with calcium ions

Simo Kalliola[a,*], Eveliina Repo[a], Varsha Srivastava[a], Juha P. Heiskanen[b], Juho Antti Sirviö[c], Henrikki Liimatainen[c], Mika Sillanpää[a,d]

[a] Lappeenranta University of Technology, Sammonkatu 12, Mikkeli FI-50130, Finland
[b] Research Unit of Sustainable Chemistry, University of Oulu, P.O. Box 3000, FI-90014, Finland
[c] Fibre and Particle Engineering Research Unit, University of Oulu, P.O. Box 4300, FI-90014, Finland
[d] Department of Civil and Environmental Engineering, Florida International University, Miami, FL-33174, USA

ARTICLE INFO

Article history:
Received 15 August 2016
Received in revised form 17 January 2017
Accepted 18 February 2017
Available online 21 February 2017

Keywords:
Carboxymethyl chitosan
Nanoparticle
Calcium
pH sensitive

ABSTRACT

In environmental applications the applied materials are required to be non-toxic and biodegradable. Carboxymethyl chitosan nanoparticles cross-linked with Ca^{2+} ions (CMC-Ca) fulfill these requirements, and they are also renewable. These nanoparticles were applied to oil-spill treatment in our previous study and here we focused on enhancing their properties. It was found that while the divalent Ca^{2+} ions are crucial for the formation of the CMC-Ca, the attractive interaction between $—NH_3^+$ and $—COO^-$ groups contributed significantly to the formation and stability of the CMC-Ca. The stability decreased as a function of pH due to the deprotonation of the amino groups. Therefore, the nanoparticles were found to be fundamentally pH sensitive in solution, if the pH deviated from the pH (7–9) that was used in the synthesis of the nanoparticles. The pH sensitive CMC-Ca synthesized in pH 7 and 8 were most stable in the studied conditions and could find applications in oil-spill treatment or controlled-release of substances.

1. Introduction

Chitin is a polysaccharide that is derived mainly from the shells of crustacean that are a waste of food industry. Chitin consists of N-acetylglucosamine monomers and it can be converted to chitosan by deacetylation of the acetyl amine groups. In chitosan the deacetylation degree (DA) is usually more than 50% i.e. over half of the monomers are deacetylated and contain primary amino groups. The reactive amino groups in chitosan, and hydroxyl groups in both chitin and chitosan, can be used for synthesizing variety of derivatives. Carboxyl groups can be introduced to the amino and/or hydroxyl groups of chitin and chitosan to enhance the solubility of the polymers in water at near neutral pH [1]. Native chitin is insoluble in water and native chitosan is soluble at pH < 7 due to the protonation of the amino groups.

Carboxymethyl derivatives of chitin and chitosan have a wide range of applications in adsorption, drug delivery, biomedicine, cosmetics, food preservatives, biosensors, and emulsion stabilization mainly due their desirable properties such as non-toxicity, biodegradability, and renewability [2,3]. One chitin/chitosan material that has received much attention in the literature is nanoparticles [4]. A major application area for polymeric nanoparticles is controlled release of drugs. Chitin and chitosan derivatives can be cross-linked into nano-scale particles with either covalent or ionic bonding. The down side of covalent cross-linking is the potentially toxic residues of unreacted cross-linkers. To avoid this, non-toxic cross-linkers such as salts may be used as ionic cross-linkers [5,6]. The non-toxicity of the materials is very important in medical applications, but it is also important in environmental applications.

Nanoparticles can adsorb to the liquid-liquid interface and stabilize emulsions. This phenomena may be applied to enhance the natural biodegradation of oil by microbes in the case of an oil-spill. The advantage of nanoparticles (>10 nm) compared to traditional molecular surfactants is that the adsorption of nanoparticles can be "irreversible" due to the surface energy reduction that can be several orders of magnitude larger than the thermal energy [7]. Traditional surfactants are in equilibrium between adsorbed and desorbed species. Desorption from the liquid-liquid interface

Abbreviations: CMC, N,O-carboxymethyl chitosan; CMC-Ca, carboxymethyl chitosan nanoparticles cross-linked with Ca ions; CMC-Na, carboxymethyl chitosan in Na-salt form; CMC-H, carboxymethyl chitosan in acid form; PDI, polydispersity index.

* Corresponding author.
E-mail address: simo.kalliola@lut.fi (S. Kalliola).

http://dx.doi.org/10.1016/j.colsurfb.2017.02.025

results in destabilization of the emulsion. Also, materials used for oil-spill treatment should be non-toxic, biodegradable, and renewable to minimize the environmental impact.

In our previous study, we used carboxymethyl chitosan nanoparticles cross-linked with Ca^{2+} ions to stabilize emulsions for applications in oil-spill treatment [8]. Carboxymethyl chitosan is non-toxic, biodegradability, and renewable, and calcium chloride is used for cross-linking due to its non-toxicity and abundance in the natural sea water. These nanoparticles can adsorb onto the oil-water interface and stabilize oil droplets in water phase. Also, the stability of these nanoparticles as a function of pH and salinity was studied and it was concluded that the nanoparticles are fairly resistant to increased salinity but are more susceptible to changes in pH. In oil-spill treatment applications, the understanding of the function of pH on the properties of these nanoparticles is relevant since the pH of the natural waters vary.

In the literature, similar carboxymethyl chitosan nanoparticles have been applied mainly to controlled-release of substances [9–13], but there is very few studies regarding the synthesis of the nanoparticles and how the synthesis conditions affect the properties of the nanoparticles [14,12]. In the literature, often the pH of the solution during the synthesis of the nanoparticles is neutral or the pH is not reported. According to our knowledge, there is no detailed studies on the effect of pH on the synthesis of these nanoparticles that would attempt to explain the nanoparticle formation mechanisms. In this paper, we studied the formation and properties of carboxymethyl chitosan nanoparticles cross-linked with Ca^{2+} ions as a function of pH to explain the previously found instability of the nanoparticles in varying pH [8]. This is important for oil-spill treatment applications and other possible applications, such as the controlled-release applications, and is useful in tuning the properties of the nanoparticles and in widening the application areas of these nanoparticles.

2. Materials and methods

2.1. Materials

Low molecular weight (50–192 kDa) chitosan (deacetylation degree 75–85%), NaOH (≥98%), and chloroacetic acid (≥99%) were supplied by Sigma-Aldrich. 2-propanol (≥99.8%) was supplied by Merck. Deuterium chloride solution (35 wt.% in D_2O, 99 atom-% D) was obtained from Sigma-Aldrich. D_2O was obtained from Eurisotop.

2.2. Synthesis of CMC

The synthesis was based on literature [1] and our previous study [8] with some modifications. One gram of low molecular weight chitosan and 1.35 g NaOH was added into a flask (100 ml) with 6 ml of water and 24 ml of 2-propanol. The mixture was stirred at 50 °C for one hour. After that, 1.5 g of chloroacetic acid dissolved in 2 ml of 2-propanol was added dropwise into the mixture while stirring. The stirring was continued for 4 h. Then, the mixture was poured into an Erlenmeyer flask and washed with ca. 700 ml of ethanol (70 v-%) followed by washing and dewatering in total with ca. 300 ml of ethanol (100 v-%). The white and slightly yellowish solid sodium salt of carboxymethyl chitosan (CMC-Na) was dried on a watch glass at room temperature. The dried CMC-Na was purified by dissolving in 50 ml of water and centrifuged at 4000 rpm for 5 min. The liquid phase was poured into 400 ml of ethanol to precipitate the CMC-Na which was separated by centrifuging at 4000 rpm for 10 min. The precipitate was washed in total with ca. 400 ml of ethanol (70 v-%), followed by washing and dewatering in total with ca. 300 ml of ethanol (100 v-%). The product was dried on a watch glass at room temperature. The dried product was ground into a fine powder using a mortar and pestle.

2.3. Synthesis of CMC-Ca nanoparticles

The synthesis of CMC-Ca was based on method reported in literature [14] but modified to be suitable for the purpose of this study. CMC-Na solutions with varying pH (7–11) were made by dissolving 50 mg of CMC-Na into 50 ml of water, adjusting the pH with 0.01 M HCl or NaOH solutions, and diluting the solution into 0.5 mg ml^{-1}. It is worth mentioning that as the CMC-Na is first dissolved in water (1 mg ml^{-1}) the pH of the solution is about 9.5 due to the basic nature of the sodium acetate groups in the polymer. The nanoparticles were synthesized by dropwise addition of $CaCl_2$ (1.5 m-%) solution into 5 ml of CMC-Na solution while stirring. The synthesis was done in a 25 ml beaker (height 50 mm, inner diameter 30 mm) with magnetic stirring bar (length 10 mm, diameter 2 mm) at 450 rpm. The volume of added $CaCl_2$ solution was varied to find the optimal conditions for nanoparticle formation in each studied pH. The formation of nanoparticles was detected by DLS measurements. The effect of NaCl (1.0 m-%) on the synthesis was studied by dissolving solid NaCl into the CMC-Na solution before the addition of $CaCl_2$.

2.4. Characterizations

The deacetylation degree (DA) of the chitosan and the substitution degree (DS) and DA of the carboxymethylated chitosan was determined with conductometric and potentiometric titrations, respectively. The presence of carboxymethyl groups in the CMC-Na was detected with FTIR-spectroscope type Nicolet Nexus 8700 (USA). The as-synthesized CMC-Na was converted to its acid form (CMC-H) [1] (Chen & Park, 2003) by suspending the solid polymer (50 mg) into a mixture of 8 ml ethanol, 2 ml of water, and 1 ml of HCl (37%). The mixture was stirred for 30 min and the polymer was washed with ethanol (80% and 100%). The sample was dried at room temperature before analysis. For ^1H NMR analyses, samples of chitosan and CMC-Na were dissolved in D_2O containing 0.7% of DCl and placed in 5 mm NMR tubes. The ^1H NMR spectra were recorded by using Bruker Ascend 400 MHz spectrometer and standard proton parameters with the delay time (d1) of 6 s at 70 °C. The nanoparticles were characterized by DLS measurements with ZetaSizer Nano ZS apparatus (Malvern Instruments Ltd.) and zeta-potential measurements were also conducted with ZetaSizer. The CMC-Ca were imaged with transmission electron microscope (TEM) Hitachi 7700 and the sizes and size distributions were determined based on the obtained images. One drop of as-synthesized CMC-Ca was placed on the sample holder grid and was allowed to dry at room temperature before imaging.

2.4.1. Determination of the deacetylation degree (DA) in chitosan

The chitosan was purified by precipitation before conductometric titration. One gram of low molecular weight chitosan was suspended in ca. 100 ml of water and HCl (~3.7%) was added slowly while stirring until the chitosan was dissolved. The pH of the solution was about 3 when chitosan was dissolved. The solution was centrifuged at 4000 rpm for 5 min to separate the undissolved impurities. Chitosan was precipitated from the separated liquid phase by increasing the pH to about 12 with 1 M NaOH solution. The precipitate was separated by centrifuging at 4000 rpm for 5 min and was washed with water several times until the solution remained approximately neutral. The precipitate was further washed with 100 ml of ethanol (70v-%) and ca. 500 ml of ethanol (100%). The product was dried on a watch glass at room temperature and ground into a fine powder using a mortar and pestle.

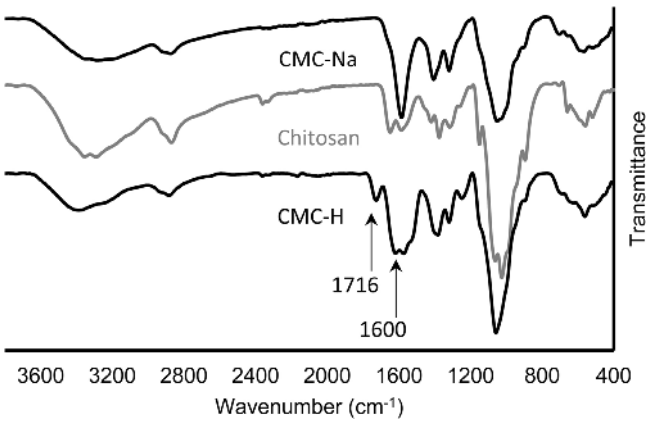

Fig. 1. FTIR spectrum of as-synthesized CMC-Na, native chitosan, and CMC-H.

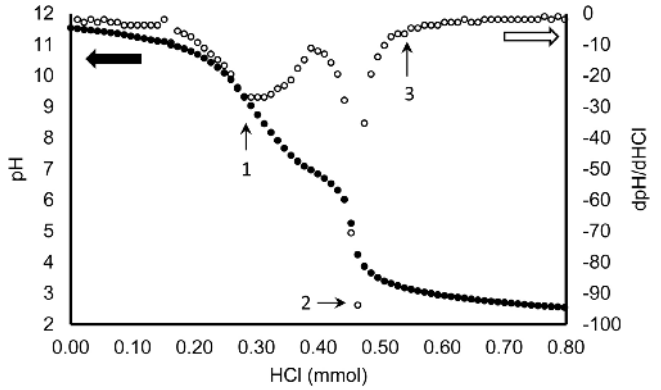

Fig. 2. Typical potentiometric titration curves of CMC-Na.

Accurately measured 50 mg of purified chitosan was suspended in 100 ml of water and HCl (~3.7%) solution was added slowly while stirring until the chitosan was dissolved. The pH was adjusted to 3 with HCl (~3.7%) solution. The solution was titrated with 0.01 M NaOH solution to pH 11 and the pH and conductance of the solution were measured as a function of added NaOH. Conductometric titrations were done in triplicates.

2.4.2. Determination of the substitution degree (DS) and DA in CMC-Na

Accurately measured 50 mg of purified CMC-Na was dissolved in 100 ml of water and the pH was adjusted to 11.5 with 1 M NaOH solution. The solution was titrated with 0.1 M HCl solution to pH 2.5, and the pH of the solution was measured as a function of added HCl. Potentiometric titrations were done in triplicates.

2.4.3. Zeta-potential measurements

A 0.5 mg ml^{-1} (50 ml) solution of CMC-Na was prepared and the pH of the solution was adjusted with HCl (0.01 M). Small samples (~0.5 ml) were taken from the solution/slurry and the zeta-potential was measured with Zetasizer.

2.4.4. Protonation of carboxyl groups

The CMC-Na was dissolved in 100 ml of water (0.5 mg ml^{-1}) and the pH was adjusted with HCl (0.01 and 0.1 M). First, the 0.1 M HCl was used to adjust the pH to ~5.9 to minimize the effects of dilution. Then, 0.01 M HCl was used to carefully adjust the pH to the desired values. Samples (~8 ml) were taken from the slurry at varying pH (3.0–5.6) and added dropwise to 35 ml of ethanol (100%) to precipitate completely. The precipitate was separated by centrifuging at 4000 rpm for 2 min and washed twice with 40 ml of ethanol to desalt and dewater the sample. Finally, the sample was dried at room temperature. The FTIR spectra were measured and the area of the band at 1716 cm^{-1} was calculated using the band at 1065 cm^{-1} as an internal standard [15].

3. Results and discussion

3.1. Characterizations of Chitosan and CMC-Na

3.1.1. FTIR analysis

The FTIR spectra of CMC-Na, chitosan and CMC-H are presented in Fig. 1.

Fig. 1. shows the FTIR spectra of chitosan and CMC-Na. After the carboxymethylation of chitosan, a broad band appears at 1600 cm^{-1} which is due to overlapping of —COONa (1598 cm^{-1}) and —NH_2 (1592 cm^{-1}) bands [1,16]. The band of —COOH group would appear at around 1720 cm^{-1} but it is not detected, indicating that the product is in sodium salt form. The FTIR spectrum of CMC-H presents a new band at 1716 cm^{-1} which is attributed to —COOH groups, confirming that the carboxymethylation was successful.

3.1.2. ^{1}H NMR analysis

The ^{1}H NMR spectra of chitosan and CMC are presented in Figs. A1 . and A2., respectively. The spectrum of CMC shows the similar characteristic proton signals as can be seen in chitosan spectrum. New signals can be found at 3.79 and 4.63 ppm which are assigned to N-CH_2-CO- and O-CH_2-CO- protons at 2- and 6-positions, respectively [17,1,18,19]. Also, three peak tops can be seen at 4.66, 4.71, and 4.77 ppm which most likely are the signals of O-CH_2-CO- protons at 3-position which overlap with the peak of D_2O. The NMR analysis confirms the successful substitution of chitosan with carboxymethyl groups.

3.1.3. Determination of DA of chitosan

Typically (Fig. A3.) the conductance of the solution is high before any NaOH was added due to the high amount of free and highly conducting H^+ ions in the solution. As the NaOH is added, the amount of free H^+ ions is decreased and the conductance is also decreased linearly. After the free H^+ ions are neutralized (pH 4.0) the protonated amino groups of chitosan start to react with NaOH and the conductance remains almost constant. When all the amino groups are neutralized (pH 8.4), the further addition of NaOH releases highly conducting OH^- ions into the solution and the conductance increases linearly. Also, the chitosan precipitates as a result of the deprotonation of the amino groups. The DA was calculated by using the two intercepts of the three fitted lines to determine the amount of deacetylated amino groups in the sample. The DA of chitosan was determined to be 78% based on three titrations. This value is in the range 75-85% that the supplier has announced.

3.1.4. Determination of DA and DS of CMC-Na

Typical pH curves as a function of added HCl are presented in Fig. 2.

In Fig. 2. the first inflection point is detected at pH 9.33 corresponding to the neutralization of excess NaOH. The CMC-Na starts to aggregate at pH ~6.8 and precipitates at pH ~5.7. The second inflection point is detected at pH 4.40 near the isoelectric point (pI) [20] where the charges of —NH_3^+ and —COO^- groups are equal. The third inflection point may be difficult to detect with potentiometric titration [21,20], but here it can be seen at pH 3.11. Based on three titrations the pK_a values for —NH_2 and —COOH groups are 7.15 and 3.40, respectively. The DA and DS values of CMC-Na were calculated by using the three inflection points. The sample was assumed to be in pure Na-salt form as detected by FTIR (Fig. 1.) and the end groups of the polymer chains were neglected. The DA and DS values were determined to be 71 and 37%, respectively. The DA value

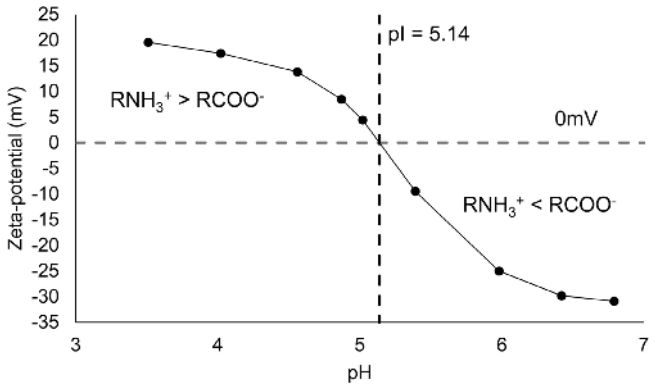

Fig. 3. Zeta-potential of CMC-Na as a function of pH.

decreased from 78 to 71% in the synthesis of CMC-Na most likely due to carboxymethylation of amino groups [1] as detected by ^{1}H NMR analysis (Fig. A2.). The DS value is low since the NaOH concentration during the synthesis was relatively low (~18 m-% in water) [1,14].

3.1.5. Zeta-potential of CMC-Na

The pI depends on the pK_a values of the two functional groups according to Eq. (1). It is assumed that the CMC-Na dissociates following Eqs. (2) and (3), additionally, all the amino and carboxyl groups are assumed to be identical. The zeta-potential measurements are presented in Fig. 3.

$$pI = 1/2\,(pK_{a1} + pK_{a2}) \quad (1)$$

$$NH_3^+RCOO^- \rightleftharpoons NH_2RCOO^- + H^+\ pK_{a1} = 7.15 \quad (2)$$

$$NH_3^+RCOOH \rightleftharpoons NH_3^+RCOO^- + H^+\ pK_{a2} = 3.40 \quad (3)$$

Fig. 3. shows that the pI of CMC-Na is 5.14 and the zeta-potential is negative above the pI due to larger amount of $-COO^-$ groups and the zeta-potential is positive below pI due to larger amount of $-NH_3^+$ groups. In comparison, the pI of the CMC-Na was determined to be 5.28 by employing Eq. (1) with the pK_a values determined from three potentiometric titrations. The pI values determined with the two different methods are in good agreement indicating that the third inflection point (Fig. 2.) is detected accurately.

3.1.6. Protonation of carboxyl groups

The aggregation of CMC-Na near the pI between pH 3.0–5.6 was exploited to study the protonation of the carboxyl groups as a function of pH with FTIR. The amount of protonated carboxyl groups depends on pH according to Eq. (4).

$$pH = pK_a + \log_{10}\left(\left[A^-\right] / [HA]\right) \quad (4)$$

The activity coefficient are assumed to be equal to 1 since the solutions are dilute. Also, since the ratio $[A^-]/[HA]$ is unitless, fractional concentrations can be used, i.e. $[A^-] + [HA] = 1$, where A^- is the deprotonated form and HA is the protonated form of carboxyl group. The FTIR spectra were measured and the area of the band at 1716 cm^{-1} was calculated using the band at 1065 cm^{-1} as an internal standard [15]. The area of the band at 1716 cm^{-1} is proportional to the amount of the carboxyl groups in the sample. By definition the amount of protonated carboxyl groups is half of the total amount of carboxyl groups at the pH corresponding to the pK_a value (3.40) of the carboxyl group, i.e. x(COOH) = 0.5 in pH 3.40. Also, x(COOH) decreases linearly as a function of pH in the vicinity of the pK_a value, allowing the area at pH 3.40 to be determined by interpolation. Therefore, the areas of the bands at 1716 cm^{-1} in varying pH were divided by two times the band area at 1716 cm^{-1} in pH 3.40 to obtain the fraction of protonated carboxyl groups. The calculation is expressed in Eq. (5).

$$x(COOH) = \left(A_{1716}/A_{1065}\right) / \left(2A_{1716,pH3.40}/A_{1065,pH3.40}\right) \quad (5)$$

Where x(COOH) is the fraction of protonated carboxylic groups at the studied pH, A_{1716} and A_{1060} are the areas of the bands at the studied pH, and $A_{1716,pH3.40}$ and $A_{1065,pH3.40}$ are the areas of the bands at pH 3.40 corresponding to the pK_a value of the carboxyl group. In Fig. 4., the experimental fractions are compared to the theoretical fractions predicted by using Eq. (4).

The Fig. 4. shows that the experimental values for the fractions of protonated carboxyl groups are in good agreement ($R^2 = 0.9890$) with the theoretical values predicted by Eq. (4). This result justifies the assumptions and confirms that the pK_a value of the carboxyl groups is close to 3.40. Also, it can be seen that all the carboxyl groups are completely deprotonated in pH ≥ 5.6.

3.2. The formation of CMC-Ca as a function of pH

The formation of CMC-Na nanoparticles without $CaCl_2$ in acidic pH was studied by adjusting the pH with HCl (0.01 and 0.1 M) and measuring the diameter and polydispersity index (PDI) values of the nanoparticles with Zetasizer. The PDI values are scaled so that a PDI value of 0.05 corresponds to a very narrow size distribution and a PDI value of 0.70 corresponds to a very broad size distribution. In pH ≥ 7, the nanoparticles were synthesized in varying pH conditions by increasing the amount of $CaCl_2$ solution (1.5 m-%) until aggregation to study the range of nanoparticle formation in each studied pH. The diameter and PDI of synthesized CMC-Ca as a function of pH and added $CaCl_2$ are presented in Fig. 5.

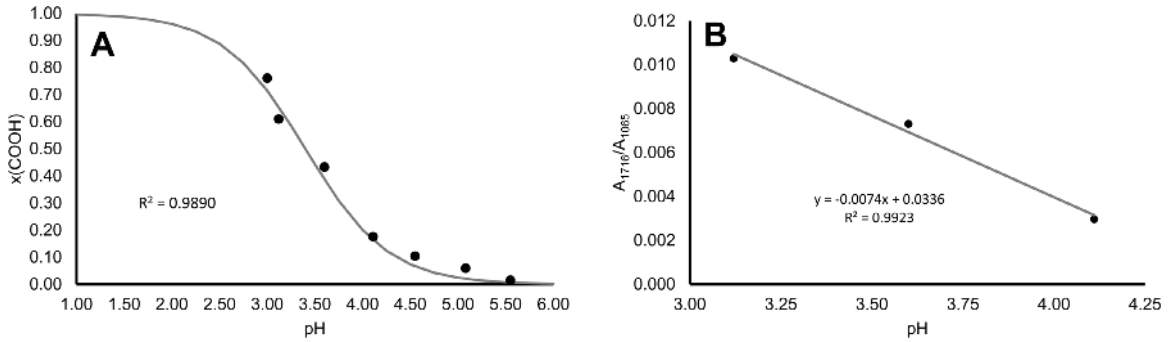

Fig. 4. A) The protonation of carboxyl groups in CMC-Na as a function of pH as detected by FTIR. The theoretical values are presented as a solid line and measured values are presented as dots. B) Interpolation of the band area in pH 3.40.

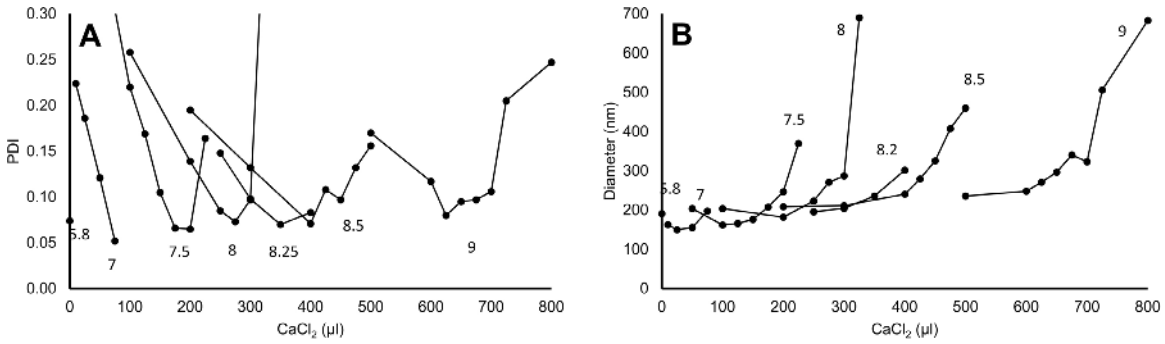

Fig. 5. A) The PDI values and B) the diameters of synthesized CMC-Ca nanoparticles as a function of added $CaCl_2$ solution in pH 5.8–9.0.

At pH ≤ 6.8 the CMC-Na solution (0.5 mg ml^{-1}) is opalescent due to the aggregation of the polymer, indicated by the decrease in the PDI value (Fig. A4). At pH 5.8 nanoparticles with PDI < 0.1 are formed just by adjusting the pH with HCl (0.1 and 0.01 M) without the addition of Ca^{2+} ions. These self-assembled nanoparticles have a PDI value of 0.074 and size of 190 nm. Similar phenomena have been described with untreated chitosan [22]. The CMC-Na precipitates at around pH 5.7 forming large aggregates, indicated by the sharp increase in the PDI value. In pH ≥ 7, the minimum PDI value and the range where nanoparticles with PDI ≤ 0.1 are formed increases as a function of pH, indicating that the size distribution of the nanoparticles is increasing towards alkaline pH, as is shown in Fig. 5. At pH 7, the nanoparticles formation range is very narrow around 75 µl of $CaCl_2$ solution and the minimum PDI value is 0.05. The CMC aggregated into large particles when 100 µl of $CaCl_2$ solution was added. At pH 9 the range is between 625 and 700 µl and the minimum PDI value is 0.08. In pH 10, nanoparticles with PDI ≤ 0.1 did not form, and in pH 11, the CMC polymer did not aggregate in the studied conditions despite the addition of $CaCl_2$ (Fig. A5). The minimum and maximum diameters of the nanoparticles also increases as a function of pH. The diameter of the nanoparticles with PDI ≤ 0.1 is close to 200 nm at pH 7. At pH 9, nanoparticles with diameter approximately between 270 to 340 nm are formed with PDI ≤ 0.1.

The increase in the required amount of $CaCl_2$ as a function of pH is in agreement with literature, where the nanoparticles were synthesized in pH 6.5–9.5 and the increase in the required amount of $CaCl_2$ was explained with zeta-potential, hydrophobic interactions and rigidity of the carboxymethyl chitosan polymer chain [12]. Based on our potentiometric titrations and FTIR measurements, the carboxylic groups (pK_a = 3.40) are completely deprotonated in pH ≥ 5.6. The amount of Ca^{2+} ions required for the nanoparticle formation should be approximately constant, if the interaction between Ca^{2+} ions and the $-COO^-$ groups would be the dominating force involved in the formation of the nanoparticles. But since the amount of Ca^{2+} ions required for the nanoparticle formation is zero at pH 5.8 and increases as a function of pH, it leads us to believe that the interaction between $-COO^-$ and $-NH_3^+$ groups plays a significant role in the formation of nanoparticles. The pK_a value of the amino groups was determined to be 7.15, indicating that half of the amino groups are protonated at this pH which supports this theory.

3.3. The role of Ca^{2+} ions and $-NH_3^+$ groups in the formation of CMC-Ca nanoparticles

The $Ca^{2+}/-COO^-$ ratio in CMC-Ca nanoparticles with PDI value ≤ 0.1 was analyzed based on the data obtained from potentiometric titrations and DLS measurements. The $Ca^{2+}/-COO^-$ ratio as a function of pH is presented in Fig. 6A). Fig. 6B) shows the fractions of $-NH_3^+$ and $-COO^-$ species and their ratio as a function of pH calculated by Eq. (4). using the pK_a values determined by potentiometric titration. The activity coefficients are assumed to be equal to 1 since the solutions are dilute and this provides good enough approximation for the purpose of this study, as shown in Fig. 4.

Fig. 6A) shows that the ratio between Ca^{2+} ions and total amount of carboxylic groups increases as a function of pH. At pH 7, the ratio of Ca^{2+} and $-COO^-$ species is 2 and the minimum ratio increases linearly until pH 8.25. At pH 8.25 there is a discontinuation point and after which the ratio increases more rapidly as a function of pH. The maximum ratio increases similarly as a function of pH, but there is more variation in the ratio. This is probably due the fact that there is an excess of Ca^{2+} ions available in the solution allowing for more possible conformations for the nanoparticles. If it is assumed that a Ca^{2+} ion would interact only with two deprotonated carboxylic groups, the ratio between Ca^{2+} and carboxylic groups would be 0.5. The ratios in Fig. 6A) are ≥2 in pH ≥ 7. These results show that a large excess of Ca^{2+} ions is required for the formation of CMC-Ca nanoparticles with narrow size distribution in pH ≥ 7 suggesting that the interaction between $-NH_3^+$ and $-COO^-$ groups is significant.

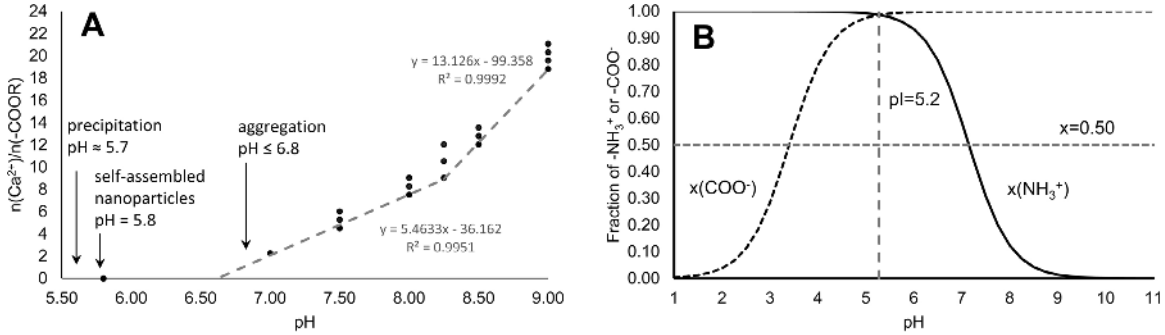

Fig. 6. A) The ratio between Ca^{2+} ions and total amount of $-COO^-$ groups as a function of pH in nanoparticles with PDI ≤ 0.1. B) The fraction of $-NH_3^+$ and $-COO^-$ groups as a function of pH.

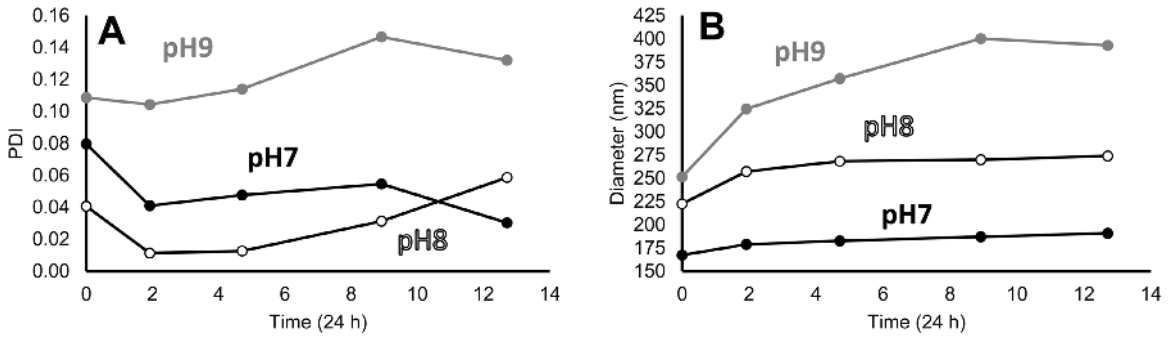

Fig. 7. A) The PDI of the as-synthesized CMC-Ca as a function of time. B) The size of the as-synthesized CMC-Ca as a function time.

Fig. 6B) shows the pK_a values of $-NH_2$ and $-COOH$ groups at pH 7.15 and 3.40, respectively, corresponding to the fraction of 0.50. The pI can be seen at pH 5.2, where the fractions of $-NH_3^+$ and $-COO^-$ species are equal (≈1.00) and the interaction between these two groups is strongest. At pH 5.80, where the self-assembled nanoparticles are formed, the fraction of deprotonated carboxyl groups is 1.00 and the fraction of protonated amino groups is ~0.95. The CMC-Na starts to aggregate at pH 6.8 where the fraction of protonated amino groups is ~0.70. Also, the fraction of $-NH_3^+$ decreases almost linearly from 0.60 to 0.07 between pH 7 and 8.25, and then diminishes slowly as a function of pH. The decrease in the fraction of $-NH_3^+$ correlates with the detected $Ca^{2+}/-COO^-$ ratios shown in Fig. 6A) indicating that as the amount of available $-NH_3^+$ groups decreases, the required amount of Ca^{2+} −ions increases to compensate the decreasing interaction between $-NH_3^+$ and $-COO^-$. The fraction of $-NH_3^+$ is approximately zero at pH 10 and 11, indicating that a negligible amount of $—NH_2$ groups are protonated and the attractive interaction between $—NH_3^+$ and $—COO^-$ groups is extremely small. In these conditions, the repulsion between $—COO^-$ groups is dominant and this could explain why CMC-Ca nanoparticles with PDI ≤ 0.1 did not form in this pH range (Fig. A5). These results suggest that the interaction between $—NH_3^+$ and $—COO^-$ groups has a significant contribution to the formation and stability of CMC-Ca nanoparticles in pH 5.8–11. Also, this shows that the nanoparticles are fundamentally unstable in solution, if the pH deviates from the pH that was used in the synthesis of the nanoparticles. These results are in agreement with our previous study [8] where we found that the CMC-Ca nanoparticles synthesized in pH 7.5 degraded in increased pH.

3.4. The effect of NaCl to the formation of CMC-Ca

The NaCl (1.0 m-%) decreases the amount of $CaCl_2$ (from 75 μl to 25 μl) required to form nanoparticles with PDI < 0.1 (Fig. A6). Although, the minimum PDI value is larger (0.09) compared to the PDI (0.05) achieved without the addition of NaCl, indicating that the size distribution increases due to the addition of NaCl. Also, the detected diameter of the CMC-Ca is significantly greater (~270 nm) compared to the samples without NaCl (197 nm). These results suggest that the hydrophobic interactions have some contribution to the formation of the CMC-Ca. The sodium and chloride ions are interacting with the CMC-Ca since the size of the nanoparticles was increased significantly. The sodium and chloride ions may induce a screening effect to carboxyl and amino groups, respectively, and enhance the hydrophobic interactions due to the decreased repulsion between the polymer chains, therefore decreasing the amount of $CaCl_2$ required to precipitate the CMC into nanoparticles. It is worth noting that the amount of Na^+ is significantly higher than Ca^{2+} in the solution (atomic ratio $Na^+/Ca^{2+} > 250$ in pH 7, PDI < 0.1), indicating that the divalent Ca^{2+} ions are crucial to the formation of nanoparticles. The synthesis of CMC-Ca in NaCl solution (1 m-%) at pH 7.5 and 8.0 did not result in nanoparticles with PDI ≤ 0.1 (Fig. A6). This could be explained by the decreased interaction between $—NH_3^+$ and $—COO^-$ groups which is further decreased by screening due to sodium and chloride ions.

3.5. The stability of as-synthesized CMC-Ca as a function of time

Three CMC-Ca samples were prepared for stability analysis in pH 7, 8, and 9, by using 75, 175, and 625 μl of $CaCl_2$ solution (1.5 m-%), respectively. The as-synthesized CMC-Ca solutions were stored in room temperature and the size and PDI of the CMC-Ca were measured with DLS as a function of time. The samples remained opalescent during the studied time. The samples were shaken gently by hand before measurements. Fig. 7 shows the PDI and size of the CMC-Ca synthesized in pH 7, 8, and 9.

The Fig. 7A) shows that the PDI of CMC-Ca in pH 7 and 8 decreases for 48 h after the synthesis and the PDI value remains <0.1 over 300 h. The PDI value of CMC-Ca in pH 9 remains approximately constant at ~1.10 for over 100 h after which it starts to increase. The Fig. 7B) shows that the size of the CMC-Ca increases as a function of time and after 48 h it saturates at 175 and 250 nm in pH 7 and 8, respectively. The size of CMC-Ca in pH 9 continues to increase until 200 h and saturates at 400 nm.

These results show that the stability of the CMC-Ca is greatly affected by pH of the CMC-Na solution and the amount of $CaCl_2$ solution used in the synthesis of the nanoparticles. The stability of CMC-Ca is better in pH 7 and 8 compared to the stability in pH 9. The CMC-Ca in pH 7 and 8 retain their narrow size distribution indicated by the low PDI value (<0.1), whereas the CMC-Ca in pH 9 has wider size distribution indicated by the higher PDI value (>0.1). Also, the average size of CMC-Ca increased in pH 9 significantly from 250 to 400 nm. The stability of the CMC-Ca seems to decrease as a function of pH, which could be explained with the decreasing interaction between $—NH_3^+$ and $—COO^-$ groups.

3.6. TEM imaging of the CMC-Ca nanoparticles

Three CMC-Ca samples were prepared for TEM imaging in pH 7, 8, and 9, by using 75, 175, and 625 μl of $CaCl_2$ solution (1.5 m-%), respectively. One droplet of as-synthesized CMC-Ca solutions were placed on the sample grid and the liquid was allowed to evaporate at room temperature before imaging. Fig. 8A) shows the TEM images of CMC-Ca nanoparticles synthesized in pH 7, 8 and 9 in dried state. The size distributions for CMC-Ca synthesized in pH 7, 8 and 9 were calculated based on several TEM images and the results are shown in Fig. 8B).

Fig. 8A) shows that the CMC-Ca synthesized in pH 7 and 8 seem spherical in dried-state but the shape of the CMC-Ca synthesized in pH 9 is more random. Fig. 8B) shows the size distributions of nanoparticles in pH 7, 8, and 9. The average sizes of nanoparticles synthesized in pH 7, 8, and 9 are 185, 283, and 306 nm, and the

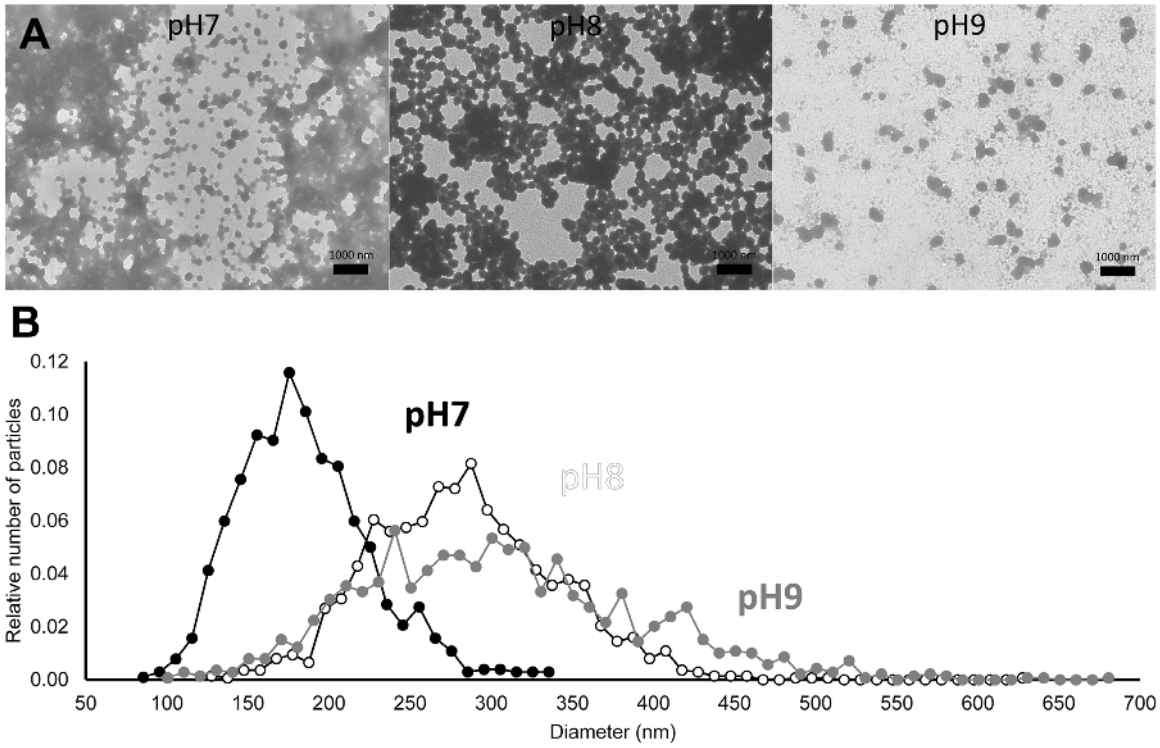

Fig. 8. A) TEM images of CMC-Ca synthesized in pH 7, 8, and 9. B) Nanoparticles size distributions determined from several TEM images in pH 7, 8, and 9. A dot represents an increment of 10 nm. The number of nanoparticles within an increment is scaled with the total number of analyzed nanoparticles in each pH. The number of analyzed nanoparticles in pH 7, 8, and 9 were 1019, 1374, and 1384, respectively.

standard deviations are 41, 57, and 85 nm, respectively. The average size and size distribution increases as a function of pH. Based on the visual analysis of the TEM images, it is possible to form spherical dried CMC-Ca with average sizes of approximately 200 and 300 nm by adjusting the pH from 7 to 8, respectively. In pH 7 and 8, the particles seem to be attached to each other after drying. In pH 9, the particles are less attached to each other, but their shape is less uniform. This may be due to degradation of the nanoparticles upon drying. Also, some non-particle matter is detected that may be dried soluble CMC due to the less stable nanoparticles in these conditions. In general, the sizes are fairly similar to those detected by DLS measurements, but the results from the two different techniques are not directly comparable. The diameter detected with DLS is the hydrodynamic diameter of the (assumed spherical) nanoparticles which deviates from the diameter in dried nanoparticles. Also, the drying process may affect the size and shape of the polymeric nanoparticles.

4. Conclusions

Nanoparticles between approximately 200 and 340 nm in size were synthesized using carboxymethyl chitosan and $CaCl_2$. The size and size distribution of the nanoparticles could be controlled by varying the pH and $CaCl_2$ concentration in the synthesis of the nanoparticles. The stability of the nanoparticles varied with the reaction conditions. The forces that contribute to the formation and stability of the nanoparticles are the interaction between $—NH_3^+$ and $—COO^-$ groups, the interaction between carboxyl groups and Ca^{2+} ions, and hydrophobic interactions. The crucial interactions are between $—NH_3^+$ and $—COO^-$ groups, and between carboxyl groups and Ca^{2+} ions. The nanoparticles synthesized in pH 7 and 8 were more stable than the nanoparticles synthesized in pH 9 in as-synthesized solutions. The increased stability in near neutral pH is attributed to the interaction between $—NH_3^+$ and $—COO^-$ groups in the carboxymethyl chitosan. The attractive interaction between these groups is stronger in near neutral pH due to the increased amount of protonated $—NH_3^+$ groups, resulting in more stable nanoparticles. Therefore, the nanoparticles are fundamentally unstable in solution, if the pH deviates from the pH (7–9) that was used in the synthesis of the nanoparticles. The nanoparticles synthesized in pH 7 and 8 can find applications in oil-spill treatment in sea water where pH is often ~8.

Acknowledgement

This study was funded by the Academy of Finland (decision number 283200).

Appendix A. Supplementary data

Supplementary data associated with this article can be found, in the online version, at http://dx.doi.org/10.1016/j.colsurfb.2017.02.025.

References

[1] X. Chen, H. Park, Chemical characteristics of O-carboxymethyl chitosans related to the preparation conditions, Carbohydr. Polym. 53 (2003), 355–259.
[2] V. Mourya, N. Inamdar, A. Tiwari, Carboxymethyl chitosan and its applications, Adv. Mat. Lett. 1 (2010) 11–33.
[3] R. Jayakumar, M. Prabaharan, S. Nair, S. Tokura, H. Tamura, N. Selvamurugan, Novel carboxymethyl derivatives of chitin and chitosan materials and their biomedical applications, Prog. Mater. Sci. 55 (2010) 675–709.
[4] R. Jayakumar, D. Menon, K. Manzoor, S. Nair, H. Tamura, Biomedical applications of chitin and chitosan based nanomaterials—a short review, Carbohydr. Polym. 82 (2010) 227–232.
[5] J. Berger, M. Reist, J. Mayer, O. Felt, R. Gurny, Structure and interactions in chitosan hydrogels formed by complexation or aggregation for biomedical applications, Eur. J. Pharm. Biopharm. 57 (2004) 35–52.
[6] J. Berger, M. Reist, J. Mayer, O. Felt, N. Peppas, R. Gurny, Structure and interactions in covalently and ionically crosslinked chitosan hydrogels for biomedical applications, Eur. J. Pharm. Biopharm. 57 (2004) 19–34.

[7] R. Aveyard, J.H. Clint, Particle wettability and line tension, J. Chem. Soc. Faraday Trans. 92 (1996) 85–89.
[8] S. Kalliola, E. Repo, M. Sillanpää, J. Arora, J. He, V.T. John, The stability of green nanoparticles in increased pH and salinity for applications in oil spill-treatment, Coll. Surf. A: Physicochem. Eng. Aspects 493 (2016) 99–107.
[9] A. Anitha, V.V. Divya Rani, R. Krishna, V. Sreeja, N. Selvamurugan, S.V. Nair, H. Tamura, R. Jayakumar, Synthesis, characterization, cytotoxicity and antibacterial studies of chitosan, O-carboxymethyl and N,O-carboxymethyl chitosan nanoparticles, Carbohydr. Polym. 78 (2009) 672–677.
[10] J. Wang, J. Chen, J. Zong, D. Zhao, F. Li, R. Zhuo, S. Cheng, Calcium Carbonate/carboxymethyl chitosan hybrid microspheres and nanospheres for drug delivery, J. Phys. Chem. C 114 (2010) 18940–18945.
[11] A. Anitha, S. Maya, K. Chennazhi, S. Nair, H. Tamura, R. Jayakumar, Efficient water soluble O-carboxymethyl chitosan nanocarrier for the delivery of curcumin to cancer cells, Carbohydr. Polym. 83 (2011) 452–461.
[12] Z. Teng, Y. Luo, Q. Wang, Carboxymethyl chitosan–soy protein complex nanoparticles for the encapsulation and controlled release of vitamin D3, Food Chem. 141 (2013) 524–532.
[13] Y.-C. Huang, T.-H. Kuo, O-carboxymethyl chitosan/fucoidan nanoparticles increase cellular curcumin uptake, Food Hydrocoll. 53 (2016) 261–269.
[14] X. Shi, Y. Du, J. Yang, B. Zhang, L. Sun, Effect of degree of substitution and molecular weight of carboxymethyl chitosan nanoparticles on doxorubicin delivery, J. Appl. Polym. Sci. 100 (2006) 4689–4696.
[15] Y. Shigemasa, H. Matsuura, H. Sashiwa, H. Saimoto, Evaluation of different absorbance ratios from infrared spectroscopy for analyzing the degree of deacetylation in chitin, Int. J. Biol. Macromol. 18 (1996) 237–242.
[16] A. Zhu, M. Chan-Park, S. Dai, L. Li, The aggregation behavior of O-carboxymethylchitosan in dilute aqueous solution, Colloids Surf. B: Biointerfaces 43 (2005) 143–149.
[17] R. Hjerde, K. Vårum, H. Grasdalen, S. Tokura, O. Smidsrod, Chemical composition of O-(carboxymethyl)-chitins in relation to lysozyme degradation rates, Carbohydr. Polym. 34 (1997) 131–139.
[18] M. Lavertu, Z. Xia, A. Serreqi, M. Berrada, A. Rodrigues, D. Wang, M. Buschmann, A. Gupta, A validated 1H NMR method for the determination of the degree of deacetylation of chitosan, J. Pharm. Biomed. Anal. 32 (2003) 1149–1158.
[19] F. de Abreu, S. Campana-Filho, Preparation and characterization of carboxymethylchitosan, Polímeros: Ciência e Tecnologia 15 (2005) 79–83.
[20] X. Kong, Simultaneous determination of degree of deacetylation, degree of substitution and distribution fraction of -COONa in carboxymethyl chitosan by potentiometric titration, Carbohydr. Polym. 88 (2012) 336–341.
[21] L. Wang, X. Chen, C. Liu, P. Li, Y. Zhou, Dissociation behaviors of carboxyl and amine groups on carboxymethyl-chitosan in aqueous system, J. Polym. Sci.: Part B: Polym. Phys. 46 (2008) 1419–1429.
[22] H. Liu, C. Wang, S. Zou, Z. Wei, Z. Tong, Simple, reversible emulsion system switched by pH on the basis of chitosan without any hydrophobic modification, Langmuir 28 (2012) 11017–11024.